Int. J. Electrochem. Sci., 13 **(2018)** 175 – 195, doi: 10.20964/2018.01.27

International Journal of
ELECTROCHEMICAL
SCIENCE
www.electrochemsci.org

Synthesis, Spectroscopic Characterization, Electrochemical Properties and Biological Activity of 1-[(4Hydroxyanilino)-methylidene] naphthalen-2(1H)-one and its Mn (III) Complex

Safia Chahmana[1], Saida Keraghel[1], Fatiha Benghanem[1,], R. Ruíz-Rosas[2], Ali Ourari[1], E. Morallón[2]*

[1] Laboratoire d'Electrochimie, d'Ingénierie Moléculaire et de Catalyse Rédox,
Département de Génie des Procédés, Faculté de Technologie, Université Ferhat
Abbas Sétif 1, Algérie.
[2] Instituto Universitario de Materiales, Universidadde Alicante, Ap. 99. E-03080 Alicante, ESPAÑA
[*]E-mail: benghanem_f@yahoo.fr

Received: 12 September 2017 / *Accepted:* 29 October 2017 / *Online Published:* 1 December 2017

The bidentate (HL) Schiff base was synthesized by reacting 2-hydroxy-1-naphthaldehyde with 4-aminophenol in absolute ethanol. The resulting HL ligand was also coordinated with the manganese ions to obtain Mn(III) complex [Mn(III)L_2ClPy (Py=pyridine)]. This Schiff base and its manganese(III) complex were characterized by multiple and usual methods including the ^{1}H NMR, ^{13}C NMR, elemental analysis (EA), FT-IR, UV-Vis, mass spectroscopy (MS), XRD, XPS and cyclic voltametry (CV). It was found that the ligand acts as a bidentate chelate. It coordinates with azomethine nitrogen and phenoxide oxygen. The other coordination sites, they are occupied by a chloride anion and a pyridine molecule completing the formation of Mn(III) Schiff base complex which is symbolized as Mn(III)L_2ClPy. Conductance values measured indicate that these compounds do not possess an electrolytic character. The electrochemical behavior of the (HL) ligand and its manganese(III) complex have been investigated using a glassy carbon electrode in the presence of 0.1 M Bu_4NClO_4 solution as a supporting electrolyte in dimethylformamide (DMF) solution. The redox system of manganese(III) complex seems to be consistent with a quasi-reversible system involving a mono electronic transfer (Mn^{III}/Mn^{II}). Both compounds, HL ligand and its Mn(III) complex were as well tested in biological activity. The obtained results indicate that they exhibit no antifungal activity but have moderate antibacterial activity towards the same organism studied. Also it is noted that this compounds have high DPPH radical-scavenging activity.

Keywords: Bidentate Schiff base ligand, Manganese(III) complex, X-Ray Analysis, XPS-analysis, Cyclic voltammetry, Biological activity.

1. INTRODUCTION

Schiff bases are known as chelating agents showing good coordinating properties. Their complexes of transition metals are very important in many domains such as catalysis, electrocatalysis and sensors where they are currently associated with the use of modified electrodes [1-4]. The non-symmetrical multidentate Schiff bases and their metal complexes have been used to inhibit the mild steel corrosion in several industrial media [5, 6]. The adsorption of such molecules depends mainly on certain physicochemical properties of the organic molecules such as the presence of nitrogen, oxygen, sulfur and phosphorus hetero atoms, or the existence of multiple bonds, as well as aromatic rings in the molecule through which they are adsorbed on the metal surface. The structural versatility of these compounds seems to be very useful for diverse applications in biology, chemistry, medicine and pharmacology [7-11]. Consequently, they have attracted considerable attention on account of their remarkable biological activities including antifungal, antibacterial and anti tumoral properties [12-19]. Some authors namely Murukan and co-workers [20], along with other studies [21, 22] have investigated the use of Schiff bases with aromatic amines and 2-Hydroxy-1-naphthaldehyde. The resulting compounds are very promising by reason of their chelating abilities with regard to the transition metal ions. Thus, many complexes of these symmetrical and non-symmetrical polydentates Schiff bases have been prepared and investigated for several purposes [10, 14, 21, 23-27]. Among all their valuable properties, it is important to highlight their photochromism and thermochromism, which are related to the probability to find these compounds in the solid state and in solution as keto-amine or phenol-imine tautomers [28-34]. Thus these aromatic Schiff bases with an o-hydroxy substituent have a very interesting property reversible color changes due to a photochromic irradiation or to a change in temperature (thermochromism). The tautomerism between the OH and NH groups yields to the change of color for thermochromic compounds. The intramolecular hydrogen transfer between an enolimine and ketoamine forms, which could be cis or trans relative to the C=N bond leads to this tautomerism. Moreover, it seems that the geometry of these molecules play an important role since the non-planar molecules can exhibit photochromism, while the planar molecules exhibit thermochromism [33]. Hadjoudis et al. [34] propose that this phenomenon may be essentially affected to the electronic density of the lone pair of the imino nitrogen atom.

In this study, we used a non-symmetrical bidentate Schiff base of manganese(III) complex, which has been scarcely studied in the literature when compared to symmetrical manganese(III) complexes, by introducing more planarity with two aromatic rings as naphthalene moiety. The non-symmetrical character will probably induce more properties such as those of biological activities. In azomethine products, the bond C=N is essential for biological activity since it is reported that several of this compounds have remarkable antibacterial, antifungal, anticancer and diuretic activities. The nature of the metal ion in Schiff bases complexes and the sequence of donor sites of the corresponding ligands affect highly the pharmacological activity of these species. In this context only few studies have been reported on such complexes with higher valence metal ions notably with Mn(III) [35-39]. Antibacterial activity of the ligand derived from 2- hydroxy-1-naphthaldehyde and its Mn(III) complexes determined show that the metal complexes have a higher or less power than the non-

coordinated ligand against the same organism under similar experimental conditions. They show moderate activity or are non toxic species [36].

The Mn(III) complexes derived from salen ligand have been successfully used as antioxidant agents [40]. The antioxidant activity of the Schiff base with aromatic group and its Mn(III) complex has been determined by the DPPH radical scavenging method. The complex exhibits greater antioxidant activity against DPPH radical than the ligand [38, 41]. Since Schiff bases derived from 2-hydroxynaphtaldehyde and aminophenol with its Mn(III) complexes revealed that they are of a particular interest. This work reports the synthesis, structural and spectral characteristics of Mn(III) complex with their electrochemical and biological studies. The non-symmetrical bidentate **(**HL**)** Schiff base is obtained by condensation of 2-hydroxy-1-naphthaldehyde on the 4-aminophenol as early described in the literature [42] and is illustrated by the following Scheme.

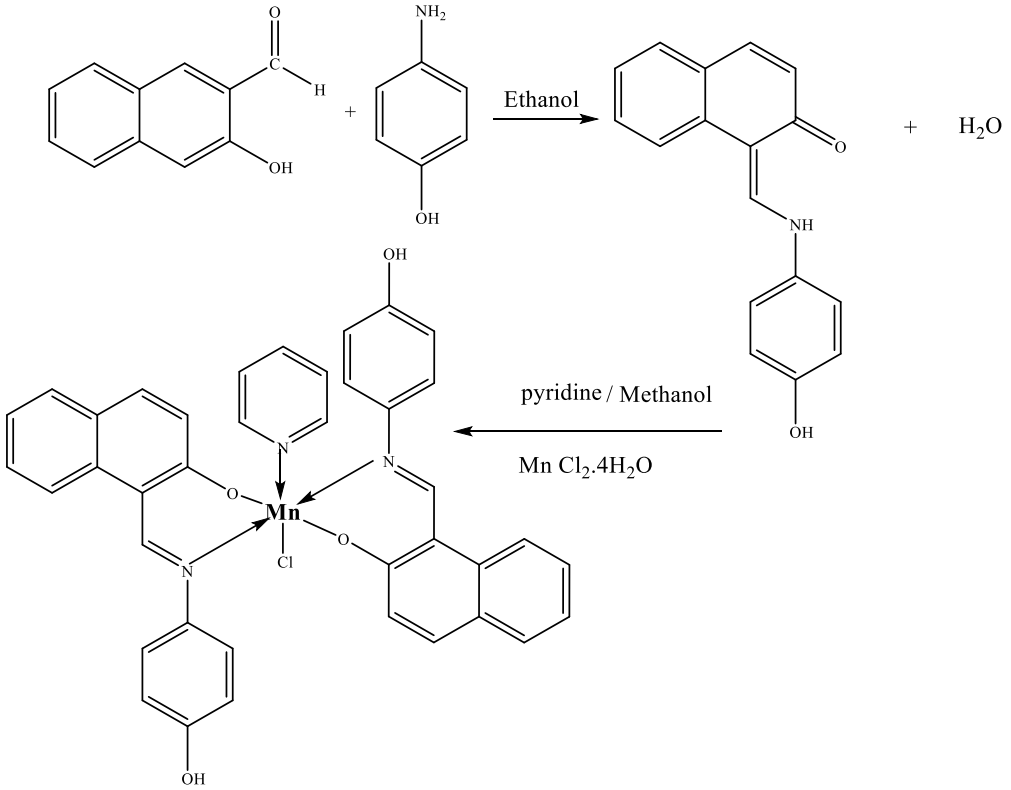

Scheme. Synthesis pathway for (HL) ligand and Mn(III)L_2ClPy complex.

.

2. EXPERIMENTAL

2.1. Materials

All chemical substances; namely: 4-aminophenol, 2-hydroxy-1-naphthaldehyde, $MnCl_2.4H_2O$, and solvents were of commercial analytical grade were purchased from Aldrich and used with no any purification.

2.2. Apparatus

The purity of the synthesized Schiff base and its Mn(III) complex was examinated by TLC using glass plates, precoated with silica gel (250 nm, Merck). A EuroVector EA3000 elemental analyzer was used for the determination of C, H, and N content of the complex. FT-IR transmission spectra were checked in the 4000-400 cm^{-1} range, using a Perkin-Elmer 1000-FT-IR spectrometer and the standard KBr pellet technique. UV–Vis measurements were obtained at room temperature using an UV-Vis 1800 UNICAM (version vision 32) spectrophotometer with standard quartz (1 cm) cells with DMF solutions of 10^{-5} M for the ligand and its complex. ^{1}H NMR and ^{13}C NMR spectra were recorded on a Bruker 400 MHz spectrometer with $CDCl_3$ or DMSO-d6 as deuterated solvents and tetramethylsilane (TMS) as the internal standard. The Mass Spectrometry analyses were realized with the HPLC Agilent 1100 series coupled to an MS with an ionic tramp detector (Agilent model 1100 Series LC/MSD Trap SL). The X-ray photoelectron spectroscopy (XPS) analyses were achieved with MULTILAB 2000 (THERMO VG) spectrometer equipped with an Al Ka X-ray source (1486.6 eV). Study was effectuated in the constant pass energy mode (100 and 20 eV, respectively). The CASAXPS program with a Gaussian–Lorentzian mix function and Shirley's background subtraction was used to deconvolute the XPS spectra. The C 1s peak at 284.6 eV was employed to correct charging effects. The analysis by the Bruker SMART APEXII CCD diffractometer was made to determine the Schiff base's crystallographic structure. The use of the Kofler Banc 7779 apparatus gave mesearment of the melting point for the Mn(III)L_2ClPy complex. The conductivity Meter MeterLab CDM-210 was been employed to determine the molar conductance of the ligand and its complex in DMF and at room temperature. The cyclic voltammograms were recorded on a Voltalab40 (potentiostat/galvanostat PGZ 301). Its electrochemical analyzer was monitored by Voltamaster4 software. The experiments were conducted under dry nitrogen conditions using conventional three-electrode single-compartment cell (5 ml).We used a glassy carbon electrode (CV) (3 mm Ø) for the working electrode. The saturated calomel electrode (SCE) and a platinum wire, were been employed as the reference electrode and the auxiliary electrode respectively. As the supporting electrolyte, we have employed the tetra-n-butylammonium perchlorate (TBAP) at 10^{-1} M. All electrochemical measurements were carried out in DMF solutions containing 10^{-3} M either for the ligand or its Mn(III) complex. These solutions were degassed with dinitrogen prior to any recording of cyclovoltammograms while maintaining them under inert atmosphere.

2.3. Preparation of the Schiff base and its manganese(III) complex

2.3.1. Preparation of the Schiff base (HL)

The Schiff base (HL) was synthesized by the condensation of 4-aminophenol on 2-hydroxy-1-naphthaldehyde. An ethanolic solution (5 ml) of 2-hydroxy-1-naphthaldehyde (0.172 g, 1 mmol) was slowly added to an ethanolic solution (5 ml) of 4-aminophenol (0.109 g, 1 mmol). The resulting solution was be maintained with stirring, under a nitrogen atmosphere, and under reflux for 5 h. A red precipitate was formed and was recrystallized from a heated ethanolic solution. A red needles was

collected and characterized using the usual physicochemical techniques (UV–Vis, FT-IR, 1H NMR, 13C NMR) and X-ray diffraction analysis. The following characteristics were found:
Yield: 60%; m.p 236°C; FT-IR (KBr, ν_x(cm^{-1})): ν_{O-H} (3443), $\nu_{(C=O)}$ (1622), $\nu_{(C=C)}$ (1543); UV-Vis (λ_{max} (nm) ε (M cm^{-1})): λ_1 (326 64900), λ_2 (340 63300), λ_3 (390 98400), λ_4 (444 47100), λ_5 (475 34700); ^{1}H NMR ($CDCl_3$, δ (ppm)): $\delta_{(C=O....HN-)}$ (1H, s, 16.07), $\delta_{(OH....N=C-)}$ (1H, s, 9.70), $\delta_{(OH)}$(1H,s, 9.60), $\delta_{(H\ arom.)}$(10 H, m, centered at 7.67); ^{13}C NMR (DMSO-d6, δ (ppm)): $\delta_{(C=O)}$ (168.95), $\delta_{(C-OH)}$ (156.66), $\delta_{(C=N)}$ (153.87) and $\delta_{(Carom)}$ (135.78-108.51).

2.3.2. Synthesis of the complex

A mixture of **(**HL**)** ligand (0.526 g 2 mmol) and an excess of pyridine in methanol was maintained under reflux for one hour. After addition of a methanolic solution of $MnCl_2.4H_2O$ (0.198 g, 1 mmol) to this mixture and after refluxing it for eight days, a dark brown solid was separated from the reaction media by filtration. Then, it is first washed with cold methanol and secondly with diethyl ether. The purity of the produced compound was checked by TLC using silica gel plates. The following characteristics were found:
Yield: 80%; m.p > 266°C; Elemental Anal. Calc.(%): C, 67.49; H, 4.21; N, 6.05; Found: C, 67.08; H, 3.71; N, 6.75; FT-IR (KBr, ν_x(cm^{-1})): $\nu_{(O-H)}$ (3427), $\nu_{(C=N)}$ (1632), $\nu_{(C=C\ )}$ (1535-1450), $\nu_{(Mn-O)}$ (672), $\nu_{(Mn-N)}$ (428), $\nu_{(Mn-Cl)}$ (400); UV-Vis (λ_{max} (nm) ε (M cm^{-1})): $\lambda_{max\ (CTLM\ )}$ (450 123000); ESI (LC-MS): $M^{+\cdot}$ = m/z 693.9.

2.3.3. Crystal structure determination of the ligand

In order to determine the structure of the (HL) ligand, we have used the X-Ray diffraction (XRD) analysis. The literature [42] describes Data collection, cell refinement, data reduction, program(s) performed to solve structure, program(s) used to refine the structure; molecular graphics and software.

2.3.4. Antibacterial experiments

The antibacterial power of the (HL) ligand and its Mn(III) complex was been tested using the agar diffusion method [43] against Escherichia coli (G-), Klebsiella pneumoniae (G-), Staphylococcus aureus (G+) and Methicillin-resistant Staphylococcus aureus (G+) species. Also, we analyzed the antifungal activity of the prepared Schiff base and its Mn(III) complex by the well diffusion method against the fungi Penicillium, Aspergillus niger, Aspergillus flavus and Fusarium oxysporum. For comparison, standard Gentamicin and Econazole (10 mg/disk) were tested as a positive control for antimicrobial and antifungal respectively. Suspensions of the bacterial strains with an optical density of McFarland 0.5 made in an isotonic sodium chloride solution were used to seed the Petri dishes of sterile Mueller–Hinton agar. Microorganisms for microbial activity were cultured 24 h at 37 °C in a nutrient agar. Sterile, 6 mm diameter filter-paper disks were impregnated with 15 µl of the tested compounds. Each compound was dissolved in dimethylsulfoxide (DMSO) in a 2.5 and 5 mg/ml

solution. Two other sterile blank disks, were used as negative controls. One is impregnated with water and the second with DMSO. Following incubation, the diameter of zones of growth inhibition was measured in millimeters. The effectiveness of the compound is estimated according the value in mm of the zone of inhibition. The fungi (10^6 spore/ml), were grown at 28 °C for seven days spread on Potato Dextrose Agar (PDA) as the medium. The wells were filled with compounds at 2.5 and 5 mg /ml concentrations. After this, the diameter of inhibition was measured.

2.4. Antioxidant activity

The aptness of the studied compounds to donate a hydrogen atom or an electron on the basis of the bleaching of the purple-colored methanol solution of 2,2-diphenyl-1-picrylhydrazyl (DPPH) was be examined with the UV–Vis spectrophotometry. This analysis (DPPH radical-scavenging activity) uses the stable DPPH radical as a reagent [44]. A quantity of 50 µL of various concentrations of the samples was mixed to 5 mL of a 0.004% solution of DPPH in methanol. The absorbance was determined against a blank at 517 nm with a Techcomp 8500 UV–Vis spectrophotometer after an incubation period of 30 min at room temperature. The percentage of the inhibition of DPPH free radical (I %) was calculated from the following equation:

$$I\ \% = [(A_{blank} - A_{sample})\ 100] / A_{blank}$$

where A_{blank} is the absorbance of the control reaction and A_{sample} is the absorbance of the analyzed compound. We determined the sample concentration providing 50 % inhibition (IC50) from a plot of I % versus concentration. Tests were performed in triplicate.

3. RESULTS AND DISCUSSION

The synthesized manganese complex was found to be mononuclear with a $Mn(III)L_2ClPy$ formula. This proposition is in perfect accordance with elemental analysis and is equally confirmed by mass spectrometry analysis for which the molecular peak ($M^{+\cdot}$) was m/z 693.9. Also, the molecular structure of the synthesized Schiff base HL was sufficiently evidenced by crystallographic studies.

3.1. Molar conductivity measurements

The HL ligand and its Mn(III) complex were dissolved in DMF and the molar conductivities of 10^{-3} M of their solutions were measured at 25 °C. The resulting values are 2.22 for the ligand and 22.13 Ω^{-1} mol^{-1} cm^2 for the complex. These values indicate that these compounds do not have an electrolytic character [45, 46].

3.2. Spectral studies

3.2.1. Infrared spectra

FT-IR spectra of the bidentate Schiff base ligand and its Mn(III) complex are given in Fig. 1**A** where the ν_{O-H} hydroxyl groups of the ligand appear as a broad 3668-3162 centered band at 3443 cm^{-1}

[47]. These frequencies express the inter- and intra-molecular interactions currently known as hydrogen bonds. The $\nu_{=C-H}$ of the aromatic rings appearing between 3090 and 3000 cm^{-1} are not clearly seen on the spectrum but, a strong absorption band, observed at 1622 cm^{-1}, is assigned to C=O (carbonyl) stretching vibration [32, 48]. In this case, it is worth to consider the solid phase of the single crystal found to be as ketonic tautomer form. The $\nu_{C=C}$ vibrational frequencies are observed in the range 1550–1450 cm^{-1} [49] suggesting a significant shifting to the lower energy due to their electronic delocalization. Fig. 1**B** shows the spectrum of the studied complex in which the main differences between the two spectra may be expected in the characteristic bonds linking the two ligand molecules to the metallic center like the absorption band of azometine, observed at 1632 cm^{-1}. This band is moved to a higher energy by about 10 cm^{-1} confirming that the Mn(III) ion is coordinated to the nitrogen atom of the azomethine mentioned above. The tautomeric equilibrium between ketoamine and enamine forms, causes some changes in the values of the frequencies, namely for the absorption bands of carbonyl and imine groups involving their possible ambiguous assignment [48]. Also other new absorption bands are observed at 672 and 428 cm^{-1} and are ascribed to (M-O) and (M-N) respectively [47, 50, 51]. Finally, the complex spectrum displayed also an absorption band at 400 cm^{-1} and is attributable to ν(M–Cl) [51]. These experimental finding are in good consistence with results reported in the bibliography for identical molecular structures.

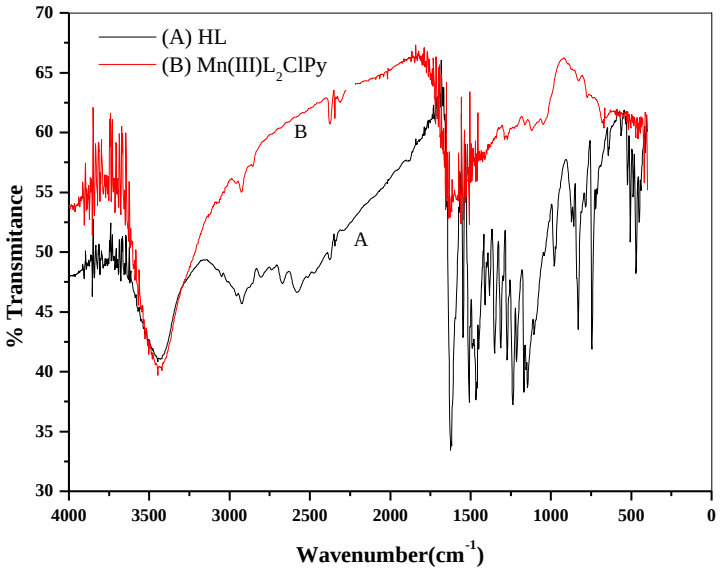

Figure 1. FT-IR spectra of **A:** (HL) ligand and **B:** its metal Mn(III)L_2ClPy complex

3.2.2. UV-VIS spectra

The electronic spectra of the **(**HL**)** ligand and its Mn(III) complex were recorded in DMF solutions (Fig. 2). In the spectrum of the ligand, five absorption bands were observed. The two first bands arising at 326 and 340 nm are attributable to **π→π*** electronic transitions associated with the naphthalene unit [21, 52, 53]. The third absorption band located at 390 nm is attributed to n→π*

transitions of conjugation between the lone pair of electrons and the conjugated π bond of the aromatic cycle [21]. The presence of bands above 400 nm such as those at 444 and 475 nm pointed out the existence of a keto-amine tautomer of the ligand [54, 55].

Concerning the electronic spectrum of the investigated complex, it shows a large absorption band at 450 nm, currently called the soret band as in porphirinic compounds [56]. It is worth to note that the intensity of this band was found to be enhanced by residual bands of its two ligand molecules observed in the same region such result is on agreement with the discussion reported in the literature [57, 58]. Thus, the transition band at 450 nm indicates that the metallic center is effectively coordinated with Mn(III) ions and expresses a charge-transfer between ligand and metal (TCLM) [59, 60]. These electronic transitions can also be associated with the azopyridine moiety (N-Pyr) [61].

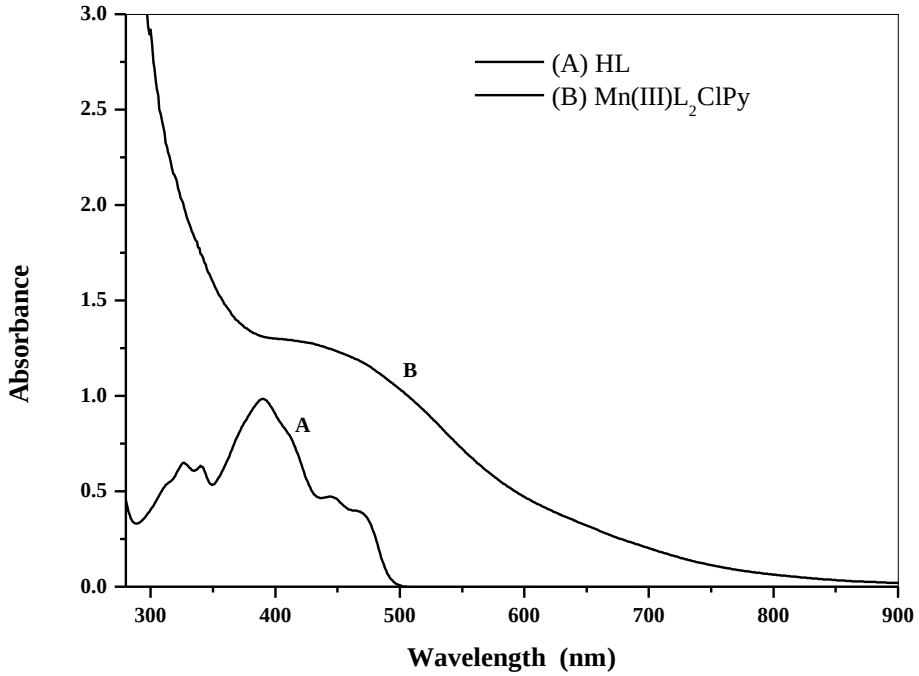

Figure 2. –Vis spectra of **A:** (HL) ligand and **B:** its metal Mn(III)L_2ClPy complex.

3.2.3. NMR spectra

Fig. 3 shows the ^{1}H NMR spectrum of the bidentate ligand. The presence of peaks at δ=16.07 ppm and δ=9.70 ppm is ascribed to amino (NH. . . .O) and enamine (=CH–NH) protons of the keto-amine tautomer [53, 54]. The peak which appeared at 9.58 ppm and whose integration corresponds to one proton is attributed to the NH group. As for the existence of peaks around 6.86–8.48 ppm, these are attributed to the aromatic protons of the ligand as reported in the literature [47, 62]. Fig. 3 also shows also the ^{13}C NMR spectrum of the same molecule on which a signal is observed at 168.95 ppm. This chemical shift is assigned to the (C=O) carbon atoms of the ketoamine tautomeric form [31]. The carbon atoms of phenolic group (C–OH) and amine one (CH-N) are observed at 153.87 ppm and

156.66 ppm, respectively [27, 31]. This spectrum displayed also other peaks between 135.78 and 108.51 ppm attributed to the carbons of the aromatic rings [27, 31].

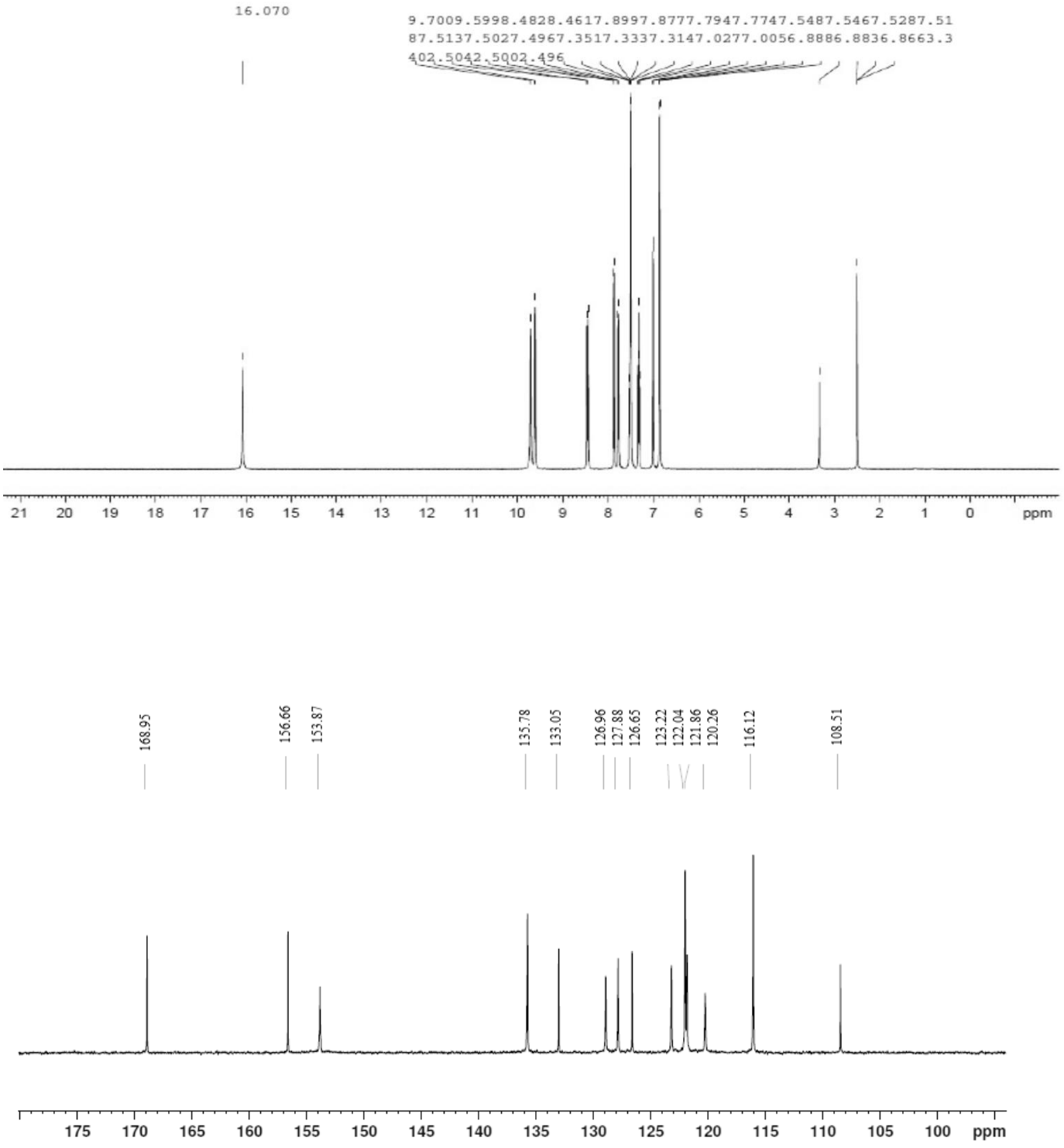

Figure 3. ^{1}H NMR and ^{13}C NMR spectra of HL ligand.

3.2.4. Mass spectrometry

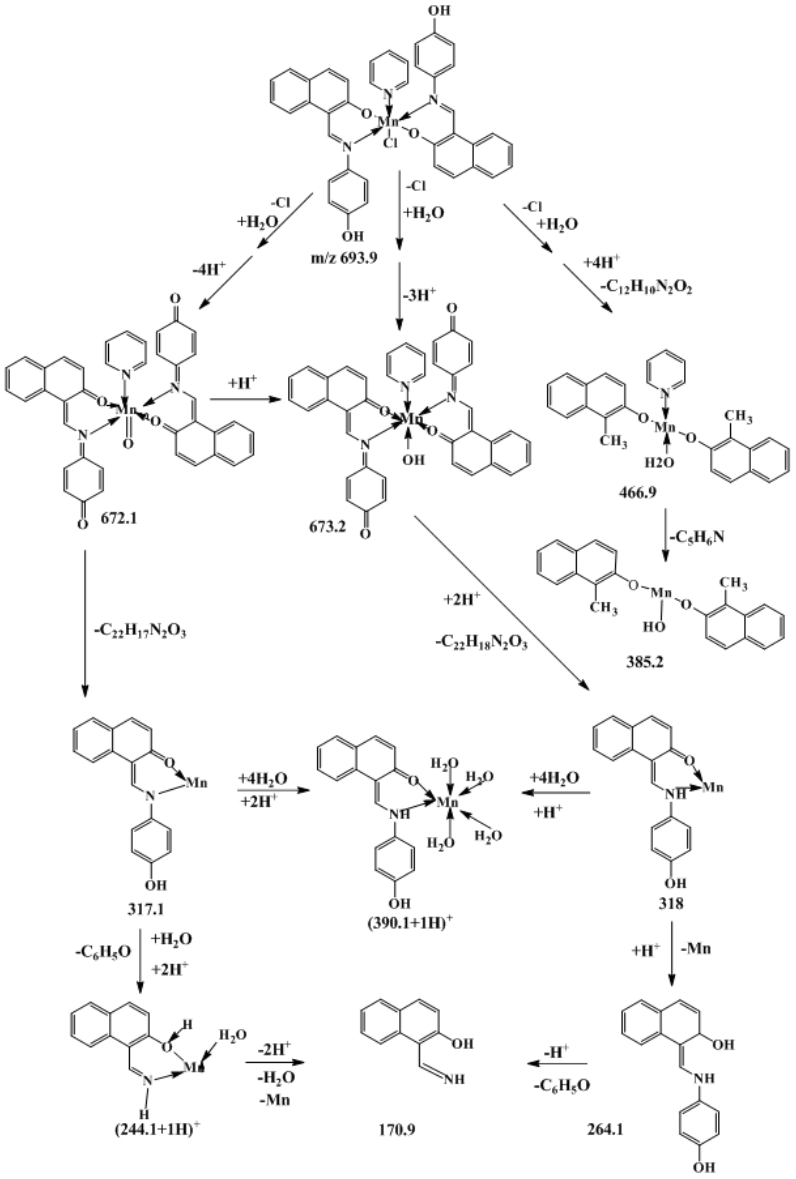

Figure 4. Main Fragmentations of Mn(III)L_2ClPy manganese-complex

The mass spectra of the manganese complex were recorded on HPLC-MS equipment using the Electro Spray Ionization technique (ESI). The resulting spectra showed the molecular peak of the manganese complex with its general formulae $[Mn(III)L_2ClPy]^{+\cdot}$. This peak was observed with a ratio m/z of 693.9 confirming the molecular weight of the expected compound. Fig. 4 illustrates the main fragments obtained from different fragmentation ways of this manganese complex. The chlorine atoms are the first lost species from the molecular form of the studied complex leading, after coordination to one water molecule, and accompanied with the loss of 3 or 4 protons yielding two cationic fragments m/z = 673.2 for $[Mn(III)L_2PyOH]^{+\cdot}$ and m/z = 672.1 for $[Mn(V)=OL_2Py]^{+\cdot}$, respectively. Furthermore, these two species lose simultaneously their pyridine molecule with one ligand (L) to give almost the same fragments as m/z = 317.1 and m/z = 318.0. These two species were tetrahydrated by a

coordination process accompanied by protonation giving the fragment of m/z = 391.2. Also the two species m/z = 317,1 and m/z = 318.0 continued their fragmentation way generating weaker molecular residues like those corresponding to m/z ratios equal to 264.1, 245.1 and 170.9. As for the phenolic entity which was not implicated in the coordination sphere of the studied complex, it was imputed from each of the two ligands, involved in the complex form, to yield m/z = 466.9 as the base peak. It seems that this fragment could be generated from a concerted mechanism stabilizing its structure by rearomatization. This species, in its turn, loses also its pyridine molecule with two protons to form the fragment with m/z = 385.2.

3.2.5. XPS Characterization

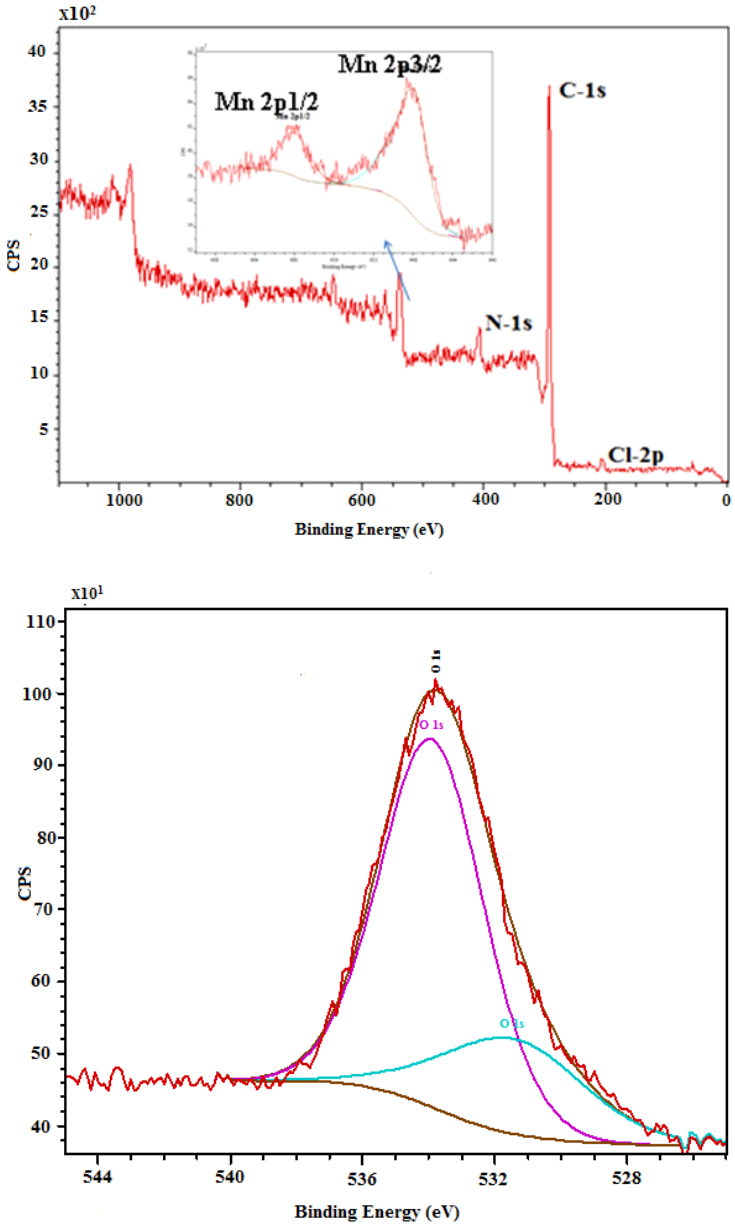

Figure 5. XPS spectra of Mn(III)L_2ClPy complex.

X-ray photoelectron spectroscopy (XPS) was used to explore the surface composition of the Mn(III) complex. The presence of Mn, Cl, C, N and O was confirmed, and their associated main peaks are shown in Fig. 5. More specifically, the O1s photoemission region appears as two components for these compounds according to the literature [63, 64]. The peaks of O1s region at 531.4 eV and 533.9 eV are attributed to the oxygen atoms of the carbonyl and hydroxyl groups (See Fig. 5). In addition, the C signal shows two peaks at 285.485 eV and at 286.6 eV that could be simultaneously assigned to C=N and C=O. The Cl 2p peak position for the Mn(III) complex was as well observed at a slightly lower binding energy at 200.8 eV. The N1s peak which is centered at 399.4 eV, is ascribed to the imine group involved in the electronic delocalization, whereas in the Mn 2p region, there are two peaks at 642.1 eV and 654.9 eV, corresponding to Mn doublet. All these binding energies can be identified with the proposed Mn(III) complex, and agree with the literature [63, 65]. The results of the XPS analysis of the surface layer concord with the sample composition.

3.2.6. Crystal structure

The zwitterionic form characterizes the crystalline structure of C17H13NO2. An intra-molecular N—H…..O hydrogen bond closes an S (6) ring. The fig. 6 shows that the Keto-amine tautomer is the favored conformation for this Schiff base in the solid state. Table 1 indicates that the short C9—O2 and C7—C8 bonds characterizes the C=O and C=C double bonds, respectively. The very short C10—C11 bond, imply the presence of a significant quinoidal effect [66-68]. The title compound is photochromic in its solid state [54]. It crystallizes in the chiral space group P212121. The dihedral angle between the planes defined by O(1)—C(1)—C(2)—C(3)—C(4)—C(5)—C(6)—N(1) and C(7)—C(8)—C(9)—C(10)—C(11)—C(12)—C(13)—C(14)—C(15)—C(16)—C(17) is equal to 14.79 (7)°. The small value of the N1—C7 bond (1.309 (3) Å) in comparison to the N1—C1 bond (1.414 (3) Å) results in a significant change in the C1—N1—C7 bond angle which is of the order of 125.97 (18) °. In the crystal, the O—H…O hydrogen bonds link the molecules into C (11) chains propagating in [010] (Table 2).

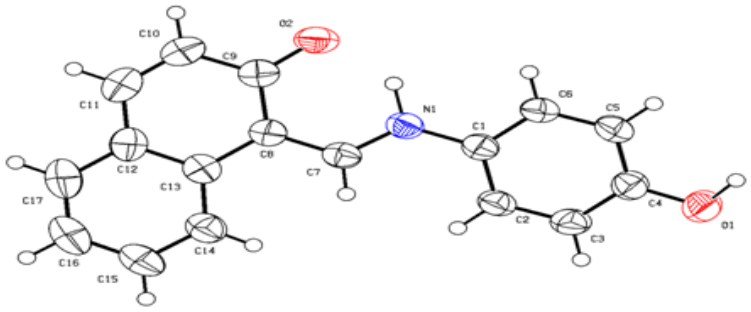

Figure 6. Molecular structure of the Schiff base, with displacement ellipsoids drawn at the 50 % probability level.

Table 1. Selected bond lengths (Å) and angles (°).

Bond lengths (Å)		Bond Angles (°)	
C1-C2	1,383 (3)	C2-C1-C6	119,00(19)
C1-C6	1,382 (3)	C2-C1-N1	122,62 (18)
C1-N1	1,414 (3)	C6-C1-N1	118,38(17)
C2-C3	1,371 (3)	C3-C2-C1	120,35(19)
C3-C4	1,384 (3)	C2-C3-C4	120,7 (2)
C4-C5	1,379 (3)	C5-C4-C3	119,2 (2)
C5-C6	1,381 (3)	O1-C4-C3	118,31 (19)
C7-N1	1,309 (3)	O1-C4-C5	122,51 (19)
C7-C8	1,399 (3)	C4-C5-C6	120,1 (2)
C8-C9	1,428 (3)	C5-C6-C1	120,61 (19)
C8-C13	1,445 (3)	C7-N1-C1	125,97 (18)
C9-C10	1,431 (3)	C8-C7-N1	124,34 (19)
C9-O2	1.286(2)	C13-C8-C7	120,38 (18)
C10-C11	1,338 (3)	C7-C8-C9	119,26 (19)
C11-C12	1,427 (3)	C10-C9-O2	120,32 (19)
C12-C13	1,412 (3)	C10-C9-C8	118,0 (2)
C12-C17	1,407 (3)	C11-C10-C9	121,5 (2)
C13-C14	1,413 (3)	C12-C11-C10	122,4 (2)
C14-C15	1,370 (3)	C13-C12-C11	118,8 (2)
C15-C16	1,386 (4)	C17-C12-C11	121,4 (2)
C16-C17	1,360 (4)	C17-C12-C13	119,8 (2)
		C14-C13-C12	117,3 (2)
		C12-C13-C8	119,01 (19)
		C14-C13-C8	123,6 (2)
		C15-C14-C13	121,3 (2)
		C14-C15-C16	120,8 (2)
		C17-C16-C15	119,7 (3)
		C16-C17-C12	121,1 (3)

Table 2. Hydrogen-bond geometry (A°,°).

D—H…..A	D—H	H…..A	D…..A	D—H….A
N1—H2N….O2	0,98 (3)	1,75 (3)	2,563 (2)	138 (2)
O1—H1A… .O2^{i}	0,89 (3)	1,80 (3)	2,680 (2)	171 (3)

Symmetry code: (i) -x; y +1/2;-z +3/ 2

3.3. Electrochemical study

The cyclic voltammetric curves of the ligand and the complex are presented in Fig. 7. The voltammogram of the (HL) ligand, recorded in the potential values ranging from -2.2V to 1.6V, shows four anodic waves at Ep_{a1}= -1.70, Ep_{a2}= 0.50, Ep_{a3}= 0.75 and Ep_{a4}= 1.07 V/SCE. The first one, observed at -1.70V/SCE, may be ascribed to the oxidized species formed during the electroreduction sweeping. The second at 0.50V/SCE, is assigned to the quinone generated from the tautomeric

equilibrium (Ketoamine-Enamine). The last two waves, located at 0.75 and 1.07V/SCE are attributed to the oxidation of amine and phenolic groups, respectively [69, 70]. For the return sweep, three cathodic waves were observed at 1.00, 0.00 and - 1.75V/SCE. The first wave corresponds to the reduced species of the oxidized amine with phenolic groups. The second wave is attributed to the quinonic reduced form at Epc_2= 0.00V/SCE while the third one is assignable to the azomethine group, reduced as observed at Epc_3= -1.65V/SCE [71, 72].

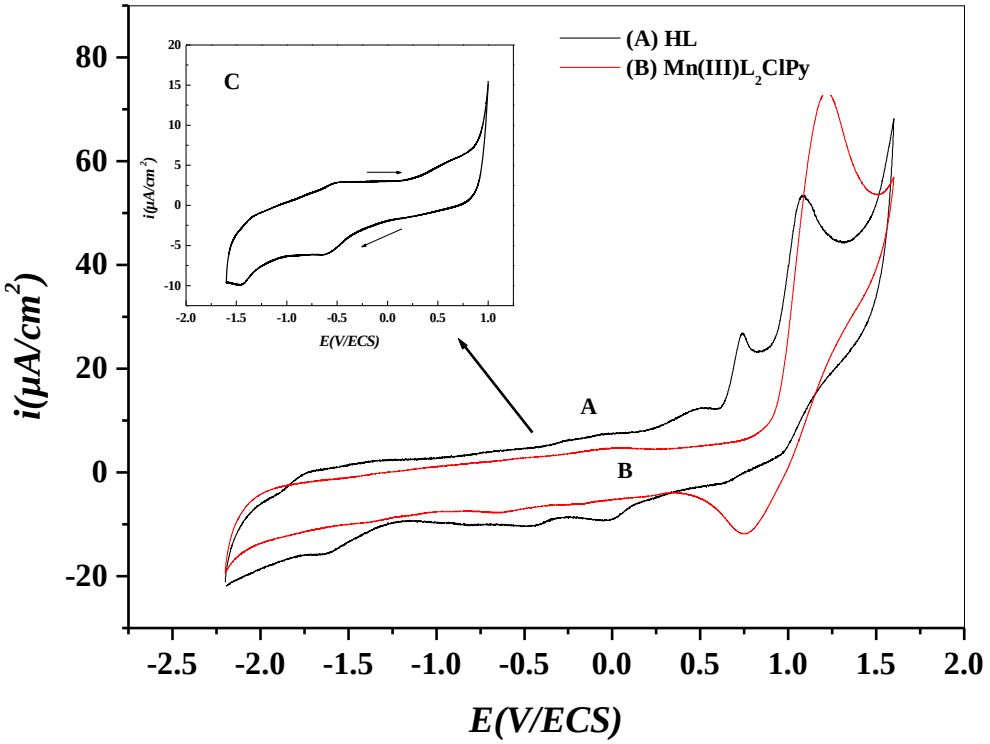

Figure 7. Cyclic voltammograms of **A:** the **HL** ligand and **B:** its Mn(III)L_2ClPy complex, **C:** cyclic voltammogram of the Mn(III)L_2ClPy in a narrower potential window; Experimental data applied for recording the three voltammograms C= 10^{-3} M in 0.1 M TBAP–DMF at v=100 mVs^{-1} with cycling from 1.6 to -2.2 V/SCE (**A** and **B**) and 1 to -1.6 V/SCE (**C**).

The Mn(III) complex exhibits one intense oxidation wave at Ep_{a1}= 1.21 V/SCE. In the cathodic side, one wave was also noted and attributed to the reduced species early oxidized. When this cyclic voltammogram is compared to those of the ligand, a disappearance of the two first waves (Ep_{a3} = 0.50, Ep_{a4} = 0.75 V/SCE) is observed. This confirms that the metal ions were coordinated to phenoxy and azomethine groups. When the potential range was limited to -1.6 - 1 V range, two anodic waves were clearly observed at Ep_{a1}= - 0.50 and Ep_{a2}= 0.60 V/SCE as shown in Fig. 7**C.** For the cathodic side, two reduction waves were also seen at Ep_{c1}= -0.62 and Ep_{c2}= -1.45 V/SCE. These waves correspond to the reduction of the Mn(III) into Mn(II) species of the complex and its azomethine group, respectively [73, 74].

The anodic signal, observed at Epa_1 =0.60 V/SCE, can probably be due to the higher oxidation state of Mn(III) to Mn(IV) [75]. The oxidation potential of the phenolic hydroxyl seems to be more positive than its value previously observed for the ligand. This fact may be related to the relative stability between the ligand and its complex. All the electrochemical characteristics were in good agreement with the spectroscopic and theoretical data. In order to study the kinetic process, the redox systems of the complex were separately investigated in the potentials range (-900-300 mV) using various scan rates (50-500 mVs^{-1}). The peak to peak separation (ΔEp = 120 mV) of the redox couple Mn(III)/Mn(II) of the complex and the cathodic intensity (i_{pc1}) increases with elevating the scan rate. The difference between forward and backward peak potentials can express the degree of reversibility of the redox system studied. The ratio of cathodic and anodic peak currents (i_{pa}/i_{pc}) was lower than unity. This ratio increases progressively to reach unity at high scan rates. The obtained electrochemical data are consistent with a quasi-reversible behavior process, typical of a monoelectronic transfer process for the first system at Epc_1=-0.62 V/SCE. The second one, noted at Epc_2= -1.45 V/SCE, is rather irreversible. The plot of the cathodic potential peak versus the log of scan rate showed a nonlinear relationship (Fig. 8). However, the peak intensity increases linearly with elevating the square root of the scan rates (Fig. 9) and with the complex's concentration. This electrochemical behavior corroborates with a quasi-reversible system controlled by diffusion [76].

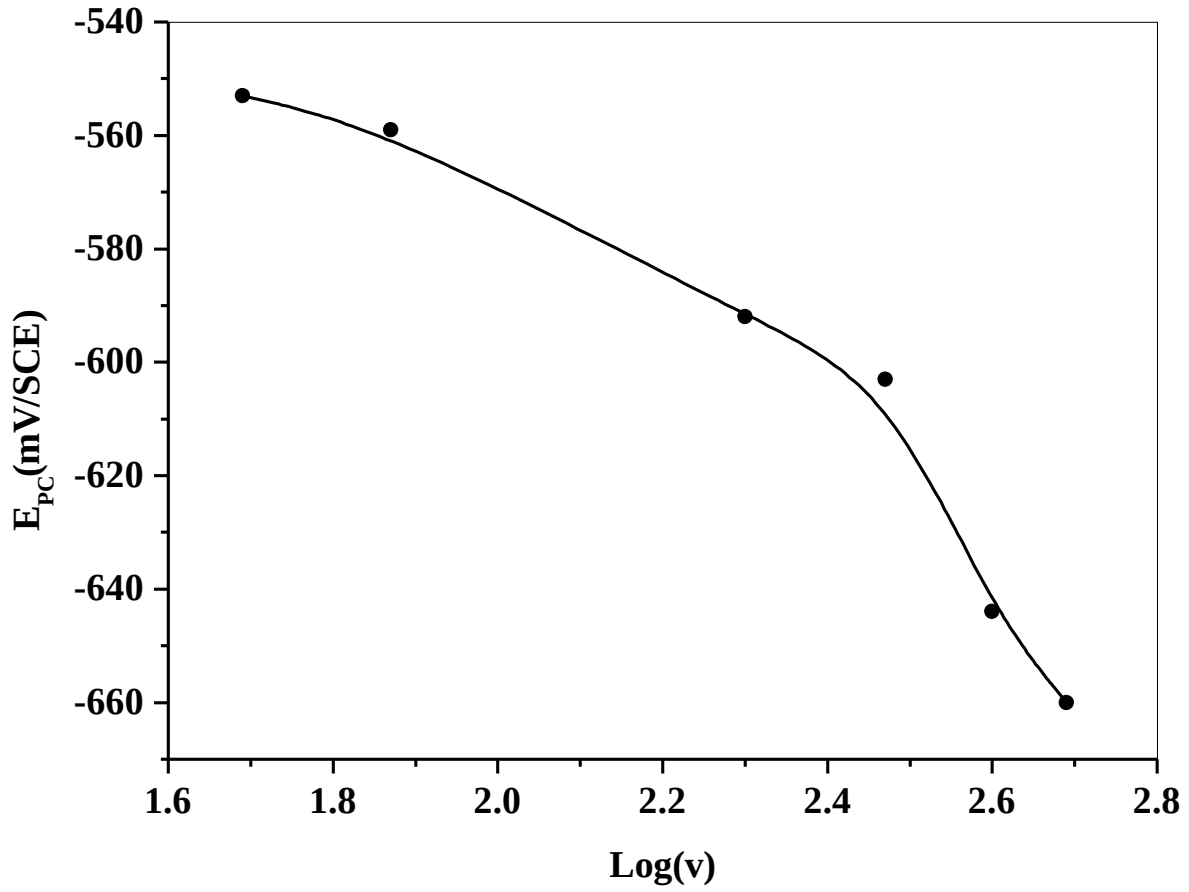

Figure 8. Plot of E_{pc} vs. log v for the Mn(III)L_2ClPy complex , C= 10^{-3} M in 0.1 M TBAP–DMF

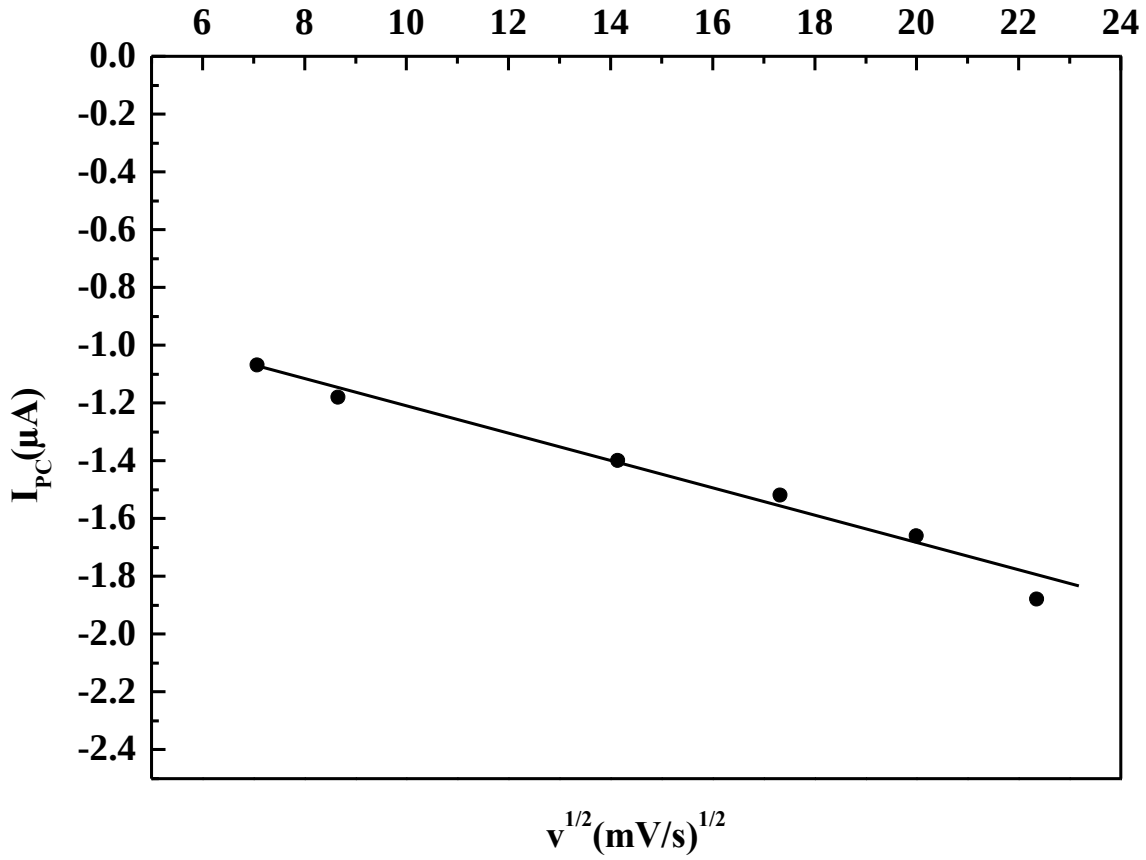

Figure 9. Plot of i_{pc} vs. $v^{1/2}$ for the Mn(III)L_2ClPy complex, C= 10^{-3} M in 0.1 M TBAP–DMF

3.4. Antimicrobial activity of the HL and the Mn(III)L_2ClPy

Currently, there is a growing interest of chemists in the field of coordination chemistry in bio-ligand synthesis using transition metals. The resulting complexes with their ligands are currently involved in extensive investigations into biological activity. It is well known that Schiff bases with diverse functional groups can give interactions with nucleoside bases. Thus, they can be favorable candidates as bactericides because they always tend to interact with some enzymes, in order to achieve a higher coordination number [20]. The hydrogen bond can occur between functional groups of the compounds and the active centers. Thus, they can interfere with the normal cell process. The antibacterial activity can be enhanced by the presence of polar substituent [20]. Aromatic Schiff bases containing the para-hydroxyl groups have a moderate inhibitory activity towards fungal strains. This kind of compounds was found to be as the most active towards antifungal and antibacterial activity [77, 78], since it has been reported in the literature that they develop important antioxidant effects due to their high capacity to intercept all sort of radicals [78]. Thus, in this paper, we attempted to study the

biological activity of our Schiff base and its Mn(III) complex. These two compounds were tested against the bacteria Escherichia coli (G^-), Klebsiella pneumoniae (G^-), Staphylococcus aureus (G^+) and Methicillin-resistant *Staphylococcus aureus* (G^+) by using the agar diffusion method [43]. The antifungal activity was also studied by the well diffusion method against the fungi Penicillium, Aspergillus niger , Aspergillus flavus and Fusarium oxysporum. The antibacterial activity of the tested compounds (HL and its complex with Mn(III)) is summarized in Table 3**.**

Table 3. Antimicrobial activity of the HL ligand and the Mn(III)L_2ClPy complex

Compounds / Microbial strains	Ligand (mg)			Complex (mg)			Gentamycin (mg)
	2.5	5	10	2.5	5	10	10
E. coli (G-)	8	8	8	7	8	9	33
Kleb (G-)	7	8	8	8	8	8	25
Staphylococcus(G+)	-	7	10	8	9	9	21
SARM (G+)	7	7	8	9	9	9	-
DMSO	-	-	-	-	-	-	-

The results revealed that the synthesized compounds exhibited close degrees of inhibition. It was found that the HL and its Mn(III) complex have moderate biological activity towards bacteria tested in these studies. When compared to the currently used standards, the results show an acceptable biological activity. In this case, it is important to note that no biological activity was observed towards antifungal organisms with our ligand and complex. The absence of the antifungal activity is probably due to the structure of the ligand associated with its steric effects, intrinsic geometry and the cell membrane of the microorganisms [36, 77-79].

3.5. Antioxidant activity of the HL and the Mn(III)L_2ClPy.

Two major mechanisms are known for an antioxidant to deactivate radicals: (a) hydrogen atom transfer (HAT) or (b) single electron transfer (SET). The 1,1-Diphenyl-2-picrylhydrazyl (DPPH) radical test affords an easy and rapid mean to evaluate the antiradical activities of antioxidants. Because that the DPPH is a stable free radical, violet-colored, and containing an odd electron in its structure, it is usually employed for the detection of the radical scavenging activity in chemical analysis. The DPPH is converted to colorless 1,1-diphenyl-2-picrylhydrazine after its reaction with the antioxidants. The degree of discoloration expresses the radical-cavenging ability of the antioxidant.

The reduction capability of DPPH radicals was evaluated from the decrease in its absorbance at 517 nm induced by antioxidants. From the plot of the percentage scavenging ability of an antioxidant versus concentration, the data were obtained [38, 80]. Inhibitory effects of the Schiff base and its Mn(III) complex on DPPH radical-scavenging activity depends on concentration (Fig.10).

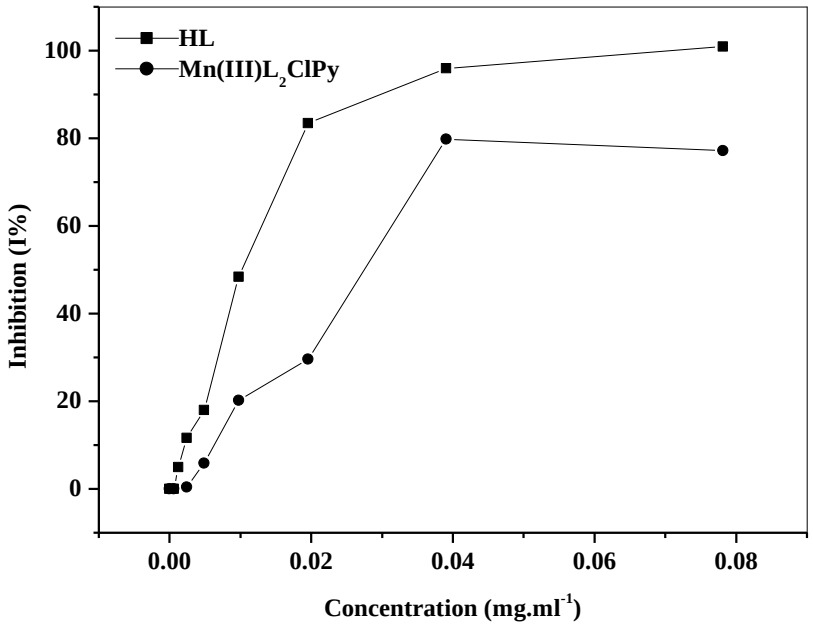

Figure 10. DPPH radical-scavenging activity of the ligand and its Mn (III) complex.

The results revealed that the Schiff base and its Mn(III) complex have good activity as a free-radical scavenger. In the present investigation, the Schiff base and its Mn(III) complex differ in their IC50 values and tendensity for scavenging free radicals (Fig.11). The ligand was more potent in eliminating free radicals than the Mn(III) complex.

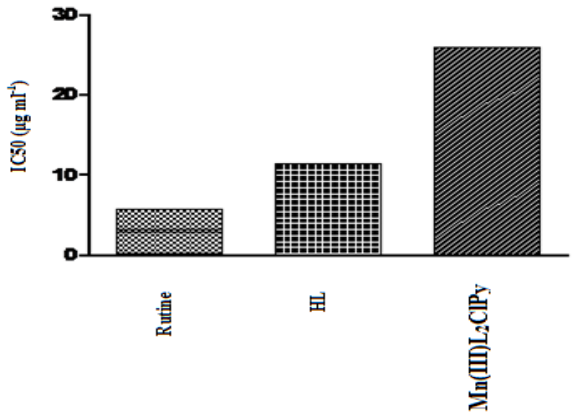

Figure 11. IC_{50} inhibitory concentration of the HL ligand and complex for 50 % of DPPH radical. Comparison was made against Rutine: $p \leq 0.001$.

4. CONCLUSION

In this work we have prepared and characterized a bidentate non-symmetric Schiff base namely 1-[(4Hydroxyanilino)-methylidene] naphthalen-2(1H)-one containing an important electronic delocalization in its molecular structure (sp^2 moieties) which improved its adsorbing and coordinating properties. This ligand was also easily coordinated with the manganese ions leading to the formation of an Mn(III) complex [Mn(III)L_2ClPy]. The electrochemical characteristics of the ligand and its manganese complex were studied and the redox system Mn(III)/Mn(II) was identified to be a quasi-reversible process. These materials tested for their performances towards biological activities such as antifungal, antibacterial and antioxidant. The results obtained indicated that the two compounds were endowed with moderate antimicrobial activity, whereas the fungal species were found to be not efficient by this treatment. However, the antioxidant activity tested against free radicals like DPPH confirmed that the ligand with its Mn(III) complex are efficient to prevent the formation of the DPPH radical. The low IC50 values, obtained for the ligand, confirms that the ligand is found to be potentially more potent to eliminate free radicals than its corresponding Mn(III) complex.

ACKNOWLEDGEMENTS
The authors gratefully acknowledge the financial support from the Algerian Ministry of Higher Education and Scientific Research. The authors would like to thank also Ministerio de Economía y Competitividad and FEDER for financial support. Thanks the Spanish Ministry of Economy and Competitiveness (MINECO) for the "Juan de la Cierva" contract (JCI-2012-12664).

References

1. A. Prakash and D. Adhikari, *Int. J. Chem. Tech. Res.*, 3 (2011) 1891.
2. A. Gorczyński, D. Pakulski, M. Szymańska, M. Kubicki, K. Bułat, T. Łuczak and V. Patroniak, *Talanta*, 149 (2016) 347.
3. B. Bouzerafa, A. Ourari, Dj. Aggoun, R. Ruiz-Rosas, Y. Ouennoughi and E. Morallon, *Res. Chem. Intermed.*, (2015) 1.
4. A.T. Fiedler and A.A. Fischer, *J. Biol. Inorg. Chem*., 22 (2017) 407.
5. R. Hasanov, M. Sadıkoglu and S. Bilgic, *Appl. Surf. Sci.*, 2 (2007) 3913.
6. M. Hosseini, S.F.L. Mertens and M. Ghorbani, *Mater. Chem. Phy.*, 78 (2003) 800.
7. A.M. Abu-Dief and I.M.A. Mohamed, *J. Basic. App. Sci.*, 4 (2015) 119.
8. J. Kumar, A. Rai and V. Raj, *Org. Med. Chem. I. J.*, 1 (2017) 1.
9. M.R. Bermejo, R. Carballido, M.I. Fernández-García, A.M. González-Noya, G. González-Riopedre, M. Maneiro and L.Rodríguez-Silva, *J. Chem.* 2017 (2017) 1.
10. S.K. Tadavi, J.D. Rajput, S.D. Bagul, J.N. Sangshetti, A.A. Hosamani and R.S. Bendre, *Mod. Chem. Appl.* 5 (2017) 1.
11. K.T. Tadele, *J. Pharm. Med. Res.*, 3 (2017) 73.
12. A.S. Munde, V.A. Shelke, S.M. Jadhav, A.S. Kirdant, S. R. Vaidya, S. G. Shankarwar and T.K. Chondhekar, *Adv. Appl. Sci. Res.*, 3 (2012) 175.
13. V.L. Chavan and B.H. Mehta, *Res. J. Chem. Environ*., 15 (2011) 57.
14. H.N. Aliyu and U. Sani, *Int. Res. J. Pharm. Pharmacol.*, 2 (2012) 040.
15. H.I. Alarabi and W.A. Suayed, *J. Chem. Pharm. Res.*, 6 (2014) 595.

16. R. Jain and A.P. Mishra, *J. Serb. Chem. Soc.*, 77 (2012) 1.
17. S.R. Morcelli, É.S. Bull, W.S. Terra, R.O. Moreira, F.V. Borges, M.M. Kanashiro, A.J. Bortoluzzi, L.L.F. Maciel, J.C.de A. Almeida, A.H. Júnior and C. Fernandes, *J. Inorg. Bio.*, 161 (2016) 73.
18. S. K. Tobriya, *Inter. J. Sci. Res*, 3 (2014) 1254.
19. M.M. Abd-Elzaher, A.A. Labib, H.A. Mousa, S.A. Moustafa, M.M. Ali and A.A. El-Rashedy, *J. basic. Appl. Sci.*, 5 (2016) 85.
20. B. Murukan and K. Mohanan, *Trans. Met. Chem.*, 31 (2006) 441.
21. A.M. Ajlouni, Z. Taha, K. Al-Hassan and A.M. Abu Anzeh, *J. Lumin*., 132 (2012) 1357.
22. B. Victory KJ, S. KU and M. Nair MK, *Res. J. Pharm. Biol. Chem.*, 1 (2010) 324.
23. A. Bagheri, N. Dastsang and K. Yari, *Der Pharmacia Lettre*, 4 (2012) 658.
24. A. Nagajothi, A. Kiruthika, S. Chitra and K. Parameswari, *Int. J. Res. Pharm. Bio. Sci.*, 3 (2012) 1768.
25. A. Bilici, I. Kaya and M. Sacak, *J. Inorg. Organomet. Polym*., 20 (2010) 124.
26. Th. Măluţan, A.P.C. Măluţan, L. Tătaru and D. Humelnicu, *J. Fluoresc.*, 18 (2008) 707.
27. M. Yıldız, E. Tan, N. Demir, N. Yıldırım, H. Ünver, A. Kiraz and B. Mestav, *Russ. J. Gen. Chem.* 85 (2015) 2149.
28. R.F. Martınez, M. Avalos, R. Babiano, P.C. Jose, L. Jimenez, M.E. Light and J.C. Palacios, *Org. Biomol. Chem.*, 9 (2011) 8268.
29. A.F. Shoair, A.R. El-Shobaky and H.R. Abo-Yassin, *J. Molec. Liquid*. , 211 (2015) 217.
30. A. Blagus, D. Cinčić, T. Friščić, B. Kaitner and V.S. Macedonian, *J. Chem. Chem. Eng*., 29 (2010) 117.
31. T.K. Venkatachalam, G.K. Pierens, P.V. Bernhardt, L. Hammond and D.C. Reutens, *J. Chem. Crystallogr*., 41 (2011) 944.
32. Z.P.G. Pavlovic, V.R.N. Dosli, D.M. Calogovic and I. Leban, *Struct. Chem*., 15 (2004) 587.
33. E. Hadjoudis, *J. Photochem*., 17 (1981) 355.
34. E. Hadjoudis, I. Argyroglou and I. Moustakali-mavridis, *Mol. Cryst. Liq. Cryst*., 156 (1988) 39.
35. Q.R. Liu, L.W. Xue and G.Q. Zhao**,** *Russ J Coord Chem*., 40 (10) (2014) 757.
36. I. Sakıyan, E. Lőgőglu, S. Arslan and N.S. Sari, N. Sakıyan, *Bio.Met.*, 17 (2004) 115.
37. G.B. Pethe, A.D. Bansod, J.B. Devhade, A.K. Maldhure and A.S. Aswar, *Res. J. Chem. Sci.*, 7 (2017) 8.
38. S.K. Tadavi, J.D. Rajput, S.D. Bagul, A.A. Hosamani, J.N. Sangshetti and R.S. Bendre, *Res. Chem. Intermed.*, 43 (2017) 4863.
39. S.K. Tadavi, A.A. Yadav and R.S. Bendre, *J. Mol. Struct.*, 1152 (2018) 223.
40. D. Bani and A. Bencini, *Curr. Med. Chem*., 19 (2012) 4431.
41. Q.M. Hasi, Y. Fan, X.Q. Yao, D.C. Hu and J.C. Liu, *Polyhedron*, 109 (2016) 75.
42. S. Chahmana, F. Benghanem, S. Keraghel and A. Ourari, *Acta. Cryst*., E70 (2014) o107.
43. AW. Bauer, WM. Kirby, J.C. Sherris and M. Turck, *Am. J. Clin. Pathol*., 45 (1966) 493.
44. W. Brand-Williams, M.E. Cuvelier and C. Berset, *Food Sci. Technol*., 28 (1995) 25.
45. A. A. Osowole, *E- J. Chem*., 5 (2008) 130.
46. W. J. Geary, *Coord. Chem. Rev*., 7 (1971) 81.
47. V. Gomathi, R. Selvameena, R. Subbalakshmi and G. Valarmathy, *Inter. J. Rech. Sci. Res*., 4 (2013) 80.
48. T. Dziembowska, M. Szafran, A. Katrusiak and Z. Rozwadowski, *J. Mol. Struct*., 929 (2009) 32.
49. M. Yıldırım and İ. Kaya, *J. Fluoresc*., 20 (2010) 771.
50. G. Ceyhan, M. Kose, V. McKee, S. Urus, A. Golcu and M. Tumer, *Spectrochim. Acta A Mol. Biomol. Spectro.*, 95 (2012) 382.
51. A.S. El-Tabl, M.M. Abd-El Wahed, M.A. Wahba, R.W. Farid and S.M.F. Hashim, *J. Chem. Bio. Phy. Sci*., A 5 (2015) 3629.
52. Z.A. Taha, A.M. Ajlouni and W.A. Momani, *J. Lum*., 132 (2012) 2832.

53. H. Temel, S. Pasaa, Y.S. Ocak, I. Yilmaz, S. Demird and I. Ozdemird, *Synthetic Metals*, 161 (2012) 2765.
54. Ö. Güngör and P. Gürkan, *Spectrochim. Acta*. A., 77 (2010) 304.
55. H. Ünver, E. Kendi, K. Güvenand and T. NuriDurlu, *Z Naturforsch*, 57 b (2002) 685.
56. C. Rimington, *Biochem*. J., 75 (1960) 620.
57. S.R. Salman and F.S. Kamounah, *Spectroscopy*, 17 (2003) 747.
58. A.A Soliman, *Spectrochimica Acta Part* A, 53 (1997) 509.
59. S. Ray, S. Konar, A. Jana, K. Das, A. Dhara, S. Chatterjee and S.K. Kar, *J. Molec. Struct*., 1058 (2014) 213.
60. S. Sasi, M. Sithambaresan, M.R. Prathapachandra Kurup and H.K. Fun, *Polyhedron*, 29 (2010) 2643.
61. S.D. Bella, I. Fragala, I. Ledoux, M.A. Diaz-Garcia and T.J. Marks, *J. Am. Chem. Soc*., 119 (1997) 9550.
62. M. MuthuTamizh, K. Mereiter, K. Kirchner, B. Ramachandra Bhart and R. Karvermbu, *Polyhedron*, 28 (2009) 2157.
63. R. Ji, K. Yu, Lan-Lan Lou, C. Zhang, Y. Han, S. Pan and S. Liu, *Inorg. Chem. Comm*., 25 (2012) 65.
64. A.R. Silva, V. Budarin, J.H. Clark, B. de Castro and C. Freire, *Carbon*, 43 (2005) 2096.
65. M. Salavati-Niasari, F. Davar and M. Bazarganipour, *Dalton Trans*., 39 (2010) 7330.
66. A. Özek, S. Yüce, C. Albayrak, M. Odabaşoğlu and O. Büyükgüngör, *Acta. Cryst*., E60 (2004) o828.
67. M. Odabaşoğlu, C. Albayrak and O. Büyükgüngör, *Acta. Cryst*., E60 (2004) o142.
68. S. Yüce, A. Özek, C. Albayrak¸ M. Odabaşoğlu and O. Büyükgüngör, *Acta. Cryst*., E60 (2004) o1217.
69. J. Niu, J. Yang Lee, A. Neudeck and L. Dunsch, *Synthetic Metals*, 99 (1999) 133.
70. A. Ourari, K. Ouari, W. Moumeni and L. Sibous, *Trans. Met. Chem*., 31 (2006) 169.
71. C. Amatore, O. Buriez, E. Labbé and J-N. Verpeaux, *J. Electroanal. Chem*., 621 (2008) 134.
72. M. Chandrasekaran, M. Noel and V. Krishnan, *J. Electroanal. Chem*., 303 (1991) 185.
73. C.K. Modi and D.H. Jani, *J. Therm. Anal. Calorim*. , 102 (2010) 1001.
74. S. Yagmur, S. Yilmaz, G. Saglikoglu, M. Sadikoglu, M. Yildiz and K. Polat, *J. Serb. Chem. Soc*., 78 (2013) 795.
75. M.S. Jana, A. K. Pramanik, D. Sarkar, S. Biswas and T.K. Mondal, *Polyhedron*, 81(2014) 66.
76. A.J. Bard and L.R. Izatt, Electrochemical Methods: Fundamentals and Applications, second ed, Wiley, New York, (2001).
77. S. Hisaindee, L. Al-Kaabi, S. Ajeb, Y. Torky, R. Iratni, N. Saleh and S.F. AbuQamar, *Arabian J.Chem*., 8 (2015) 828.
78. N. Vukovic, S. Sukdolak, S. Solujic and N. Niciforovic, *Synth. Vitro. Asse. Food. Chem*., 120 (2010) 1011.
79. S.M. Abdallah, M.A. Zayed and G.G. Mohamed, *Arabian J. Chem*., 3 (2010) 103.
80. R.L. Prior, X. Wu and K. Schaich, *J. Agric. Food Chem*., 53 (2005) 4290.